UNITED STATES DEPARTMENT OF THE INTERIOR

GEOLOGICAL SURVEY

Temperature, thermal conductivity, heat flow, and radiogenic heat production from unconsolidated sediments of the Imperial Valley, California

by

J. H. Sass[1], S. P. Galanis, Jr.[2], A. H. Lachenbruch[2],

B. V. Marshall[2], and R. J. Munroe[2]

Open-File Report 84-490

This report is preliminary and has not been reviewed for conformity with U.S. Geological Survey editorial standards and stratigraphic nomenclature.

[1]Flagstaff, Arizona [2]Menlo Park, California

1984

Table of Contents

Abstract

A combination of in situ and conventional heat-flow determinations, re-evaluation of some published data, and estimates from gradient wells and from two deep test wells resulted in a total of 322 heat-flow determinations for the unconsolidated sediments of the Imperial Valley. Temperature gradients from industry gradient wells were combined with the regional mean of 93 in situ determinations of thermal conductivity (1.88 $Wm^{-1} K^{-1}$ ± 0.34 SD) to obtain heat-flow estimates. The availability of a suite of drill cuttings from a 2.5 km test well at El Centro together with a suite of geophysical logs including velocity and porosity logs allowed an independent test of the empirical Goss-Combs relations between thermal conductivity and seismic velocity and density. The relations fit very well at the high-velocity high-conductivity (>2.5 km s^{-1}, >1.7 W $m^{-1} K^{-1}$) end, but require modification for lower velocities and conductivities, where Goss and Combs had no data. To take account of an irregular geographical distribution of data, heat-flow data were averaged within 3' × 3' (~5 × 5 km) elements; the mean of 99 such elements was 166 mW m^{-2} ± 97 (SD). If the ten elements with average heat flows >280 mW m^{-2} (associated in each instance with known near-surface hydrothermal convection systems) are excluded, the overall mean conductive heat flow for the Imperial Valley is 139 mW m^{-2} ± 46 (SD).

INTRODUCTION

The Imperial Valley (Figure 1) comprises the northern part of the Salton Trough, a tectonic depression at the northern end of the Gulf of California. It is also the southern terminus of the San Andreas transform system. In a recent series of reports (Lachenbruch and others, 1983a, 1983b, 1984), we have sought to explain the thermal regime of the Imperial Valley and its surrounding terranes in terms of steady-state thermo-mechanical models involving extension, intrusion or accretion of basalt, subsidence and sedimentation. Details of the thermal regime of the surrounding crystalline terranes are presented by Lachenbruch and others (1984). In this report, we present 322 estimates of heat flow from the unconsolidated sediments of the Imperial Valley, together with supporting temperature, thermal conductivity, and heat-production data.

The heat-flow data (Figure 2) consist of: 1) 15 heat flows published by Mase and others (1981) for the Glamis - East Brawley area (Figure 1); 2) an additional 11 values obtained in the Central and Western Imperial Valley--both of these data sets were obtained using the in situ technique described by Sass and others (1979, 1981); 3) temperature data from 260 temperature-gradient wells were obtained from Republic Geothermal, Inc. (R. W. Rex, personal communication, 1983). Temperature gradients below 60 m were combined with the mean thermal conductivity obtained in situ (1 and 2 above) to obtain estimates of conductive heat flux (Figure 2); 4) heat flow at 34 sites in the East Mesa area (Figures 1 and 2) for which data were originally published by Swanberg (1974a, 1974b) was re-evaluated by combining the least-squares gradients below 46 meters with the mean in situ conductivity; 5) data from two deep wells near El Centro (Figure 2) were used to estimate heat flow.

Acknowledgments. We are indebted to R. W. Rex for supplying unpublished gradient data and to A. R. Smith for determinations of radiogenic heat production. Assistance in the field was provided by J. P. Kennelly, Jr., T. H. Moses, Jr., and E. P. Smith. C. A. Swanberg and W. H. Diment made constructive comments on an early draft.

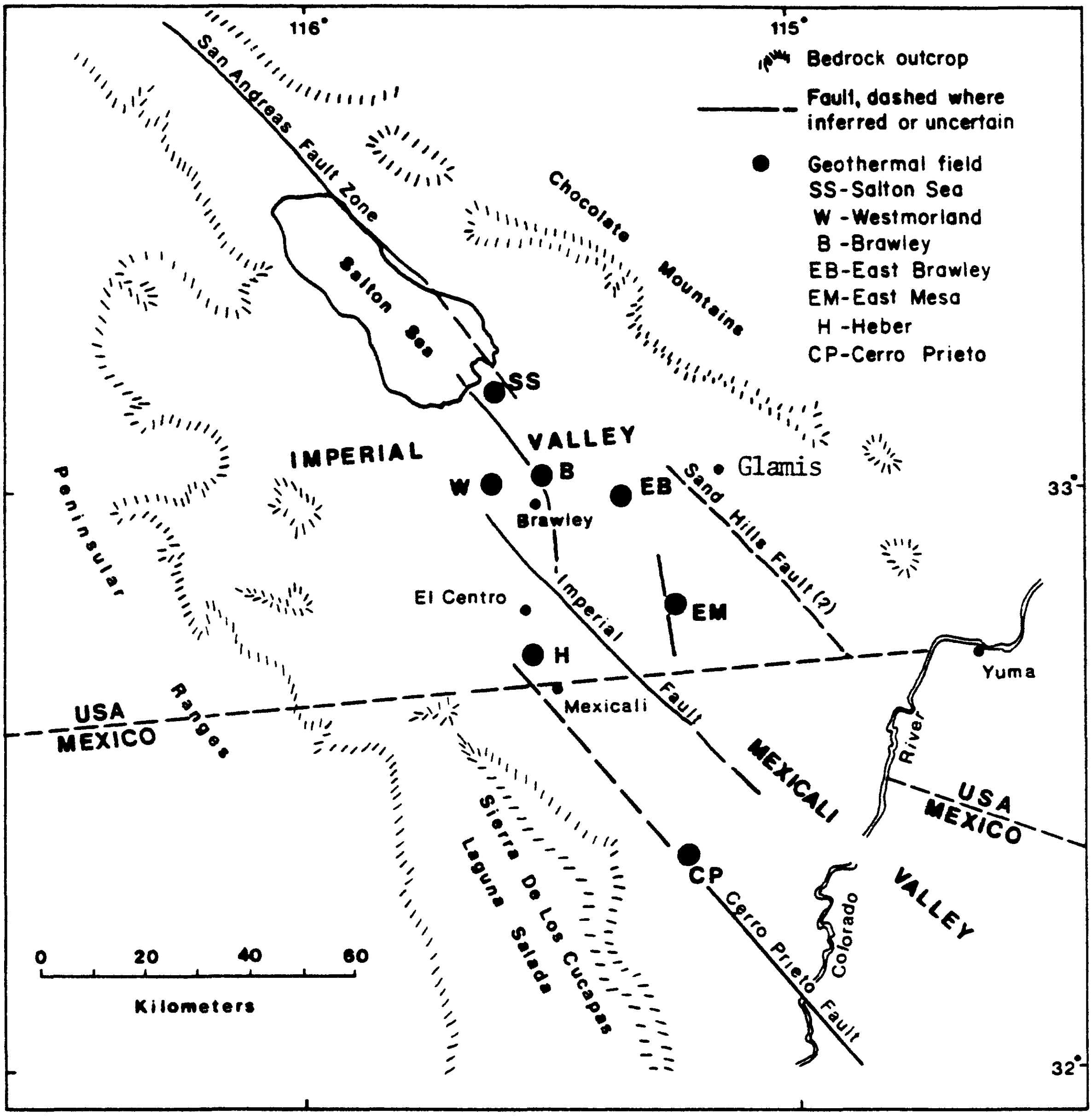

Figure 1. Map of the Imperial and Mexicali Valleys showing locations of known geothermal fields and selected faults (from Mase and others, 1981).

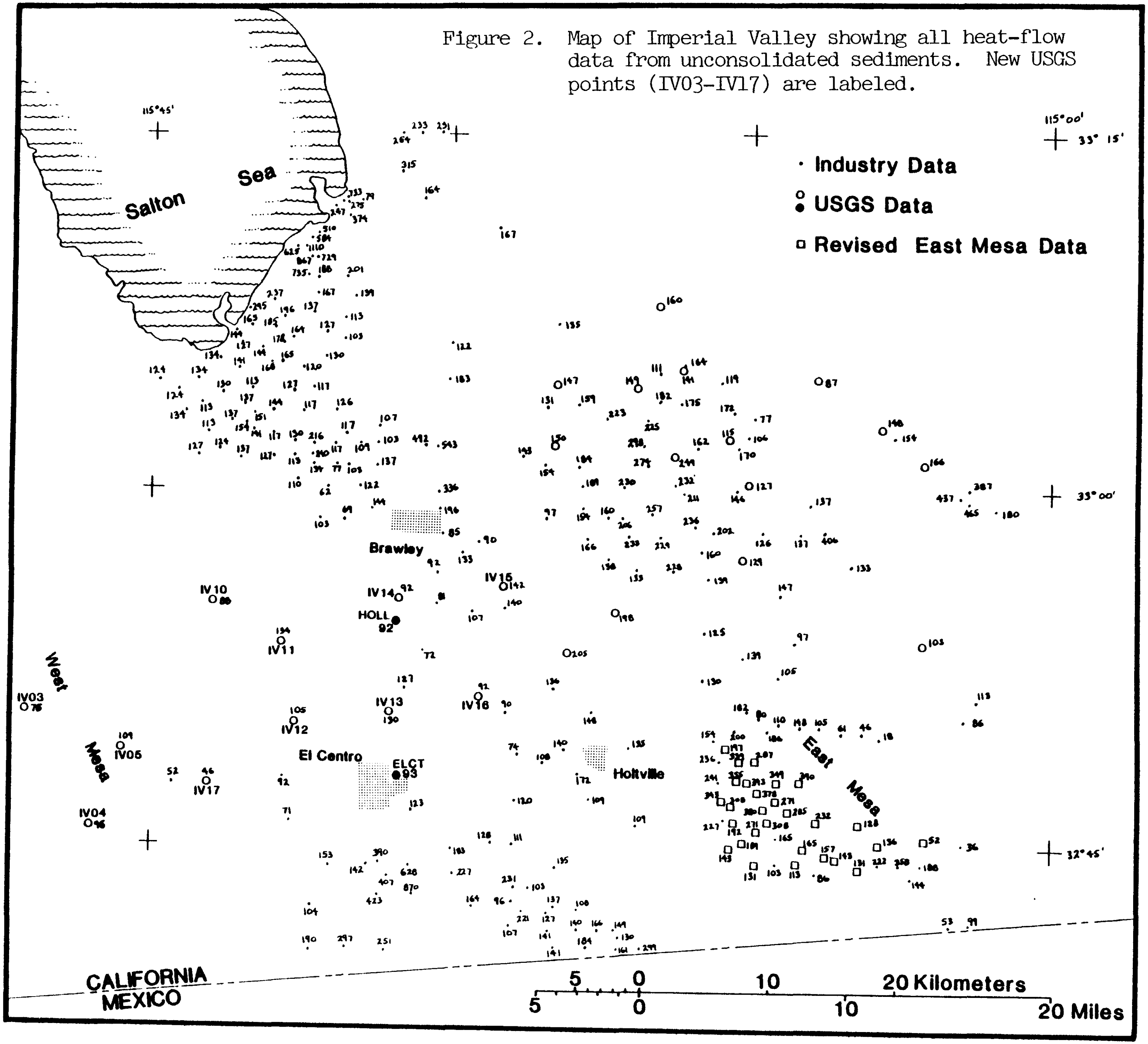

Figure 2. Map of Imperial Valley showing all heat-flow data from unconsolidated sediments. New USGS points (IV03-IV17) are labeled.

NEW HEAT FLOWS

To fill in some obvious gaps in geographical coverage, 11 sites labeled IV03 through IV17 (Figure 2) were drilled during May of 1983, and in situ temperature and thermal conductivity determinations were attempted using the technique described by Sass and others (1979, 1981) at various depths. Based on the experience of Mase and others (1981) in the Glamis - East Brawley geothermal fields (Figure 1), downhole probe runs were made initially at 60 m, then 90, 120, and sometimes, at 140 m. Because of mechanical problems with the probe system, we were unable to achieve the necessary penetration beyond the drill bit in IV03. In IV04, the drill encountered highly silicified partly consolidated material which could not be penetrated by the downhole probe. For these sites, casing was left in the wells for later conventional temperature logs, and thermal conductivities were estimated from laboratory measurements on drill cuttings.

A composite diagram illustrating temperature profiles in all 11 wells is presented in Figure 3. Continuous temperature logs obtained about a month after drilling are shown for wells IV03 and IV04. Each of the remaining profiles comprises the three or four discrete temperatures obtained during drilling joined by straight line segments. Extrapolated surface temperatures range from ~24 to 27 °C. For convenience in assessing individual profiles, the temperature data are plotted with arbitrary temperature scale in Figure 4.

A total of 44 in situ determinations of thermal conductivity were obtained (Table 1). The distribution of values is bimodal (Figure 5), corresponding to alternating layers of sandy and relatively clay-rich sediments. The mean conductivity of 1.89 ± 0.33 (SD) is intermediate between the modes of ~1.6 and 2.25 $W\ m^{-1}\ K^{-1}$, both the distribution and mean are similar to those for the Glamis - East Brawley area (Figure 6) so that we combined the two data sets (Figure 7) to derive a mean value of 1.88 ± 0.34 (SD) for the unconsolidated sediments in the upper ~200 m of the Imperial Valley.

Thermal conductivities were also measured on drill cuttings from the various wells using the "chip" technique of Sass and others (1971). Individual conductivity-depth pairs are presented in Table 2, and the distribution of values is illustrated in the histogram of Figure 8. Once again, the distribution is similar to that found in the Glamis - East Brawley region (cf., Figure II-1 of Mase and others, 1981), and the means are comparable (2.88 ± 0.57 (SD) $W\ m^{-1}\ K^{-1}$ versus 3.03 ± 0.73 for Glamis). The samples were sieved (~100 mesh) and washed from the flow line during drilling. Possible systematic errors in grain conductivities might arise from both contamination by drilling mud and loss of fines to the drilling mud. We have no way of assessing precisely the magnitude of such errors; however, studies of both core and cuttings from other areas (e.g., Sass and others, 1977) suggest that they amount to no more than a few percent.

No independent determinations of formation porosity were made. We were, however, able to "back out" values of porosity by assuming that the in situ thermal conductivity (K_f, Table 1) was related to the corresponding grain

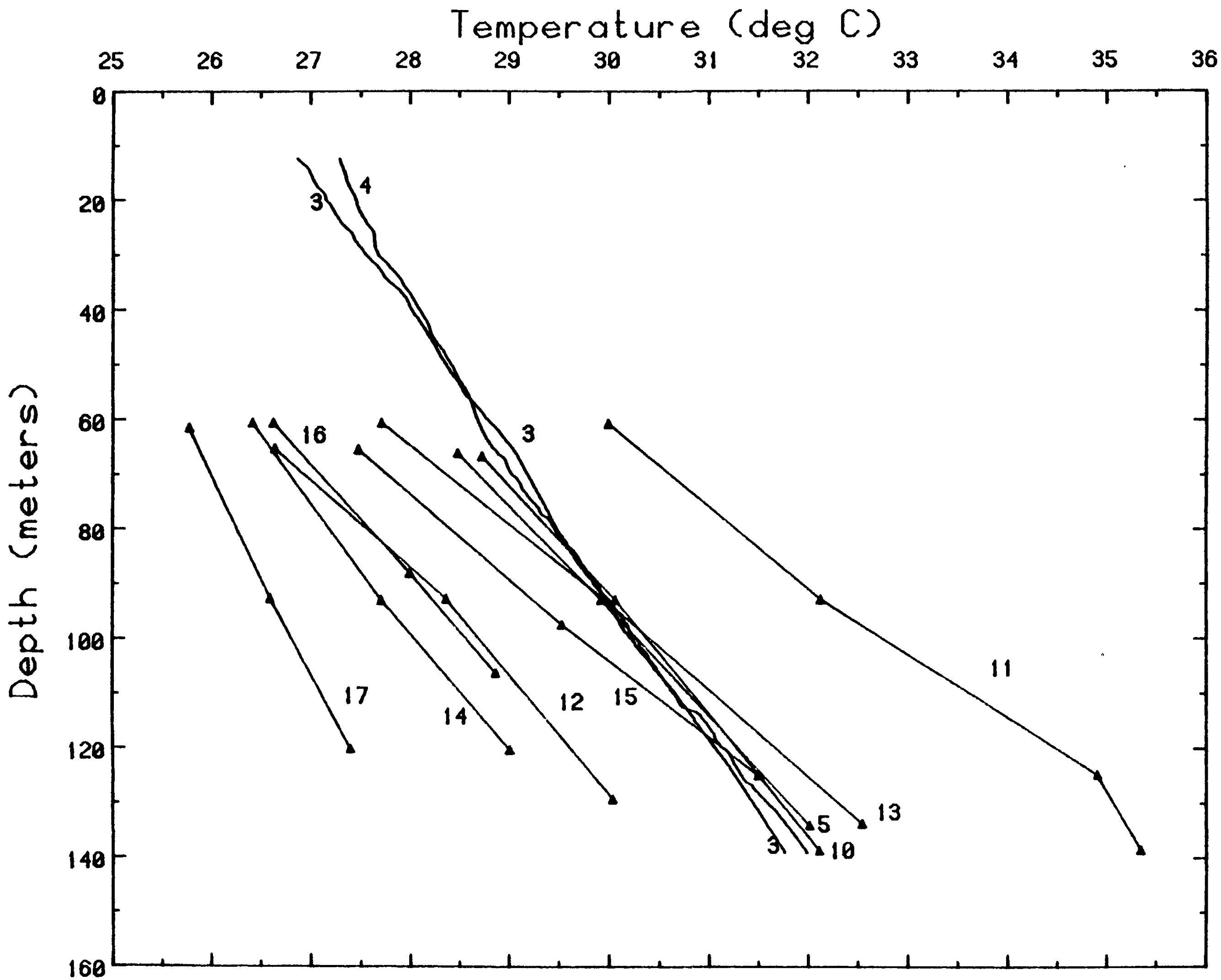

Figure 3. Temperature profiles for 11 wells in the Central and Western Imperial Valley (Figure 2).

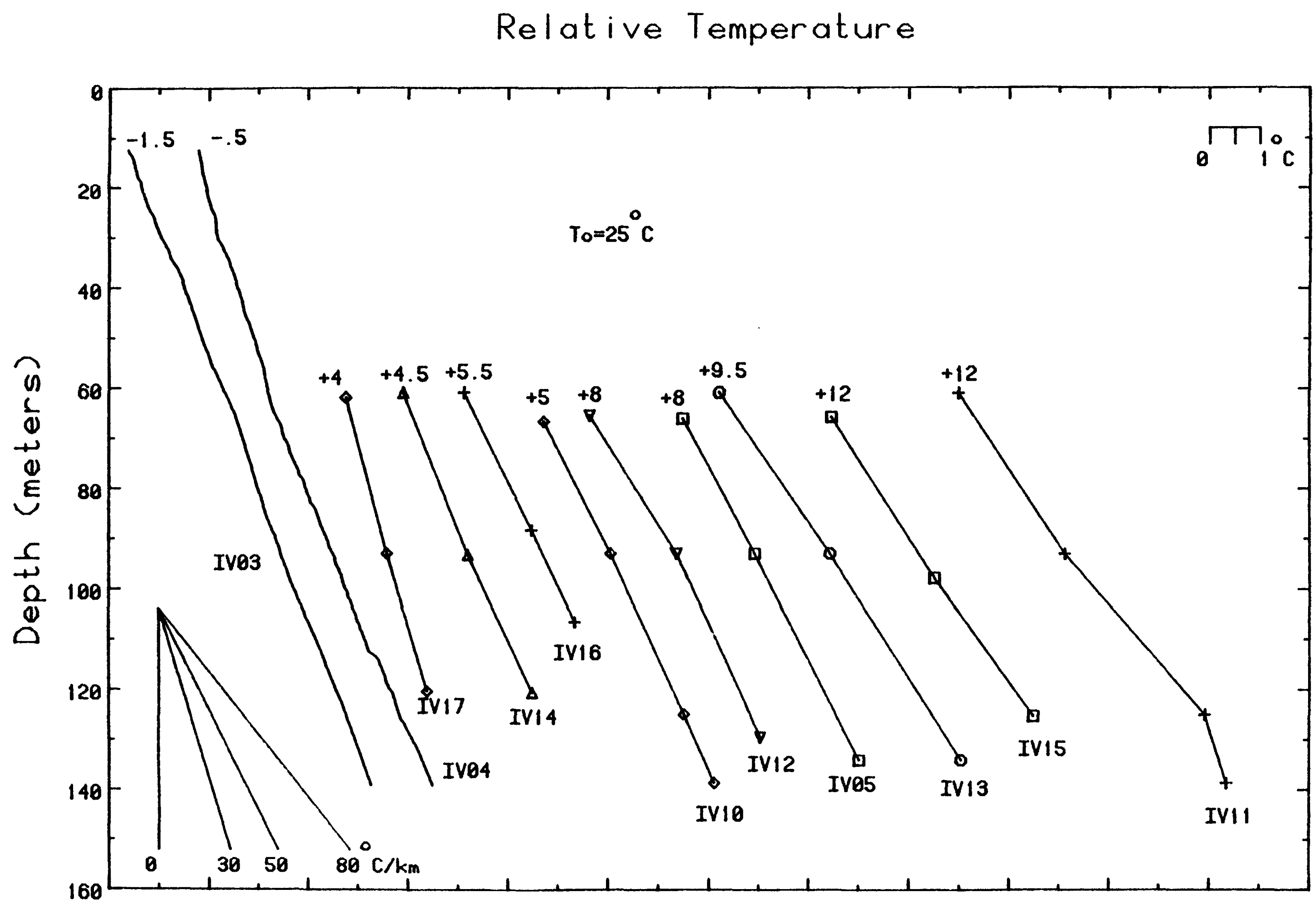

Figure 4. Temperature profiles of Figure 3 replotted with arbitrary temperature origin. Numbers above and to the right of profiles denote the amount of rightward shift (in °C) relative to a temperature origin of 25°C.

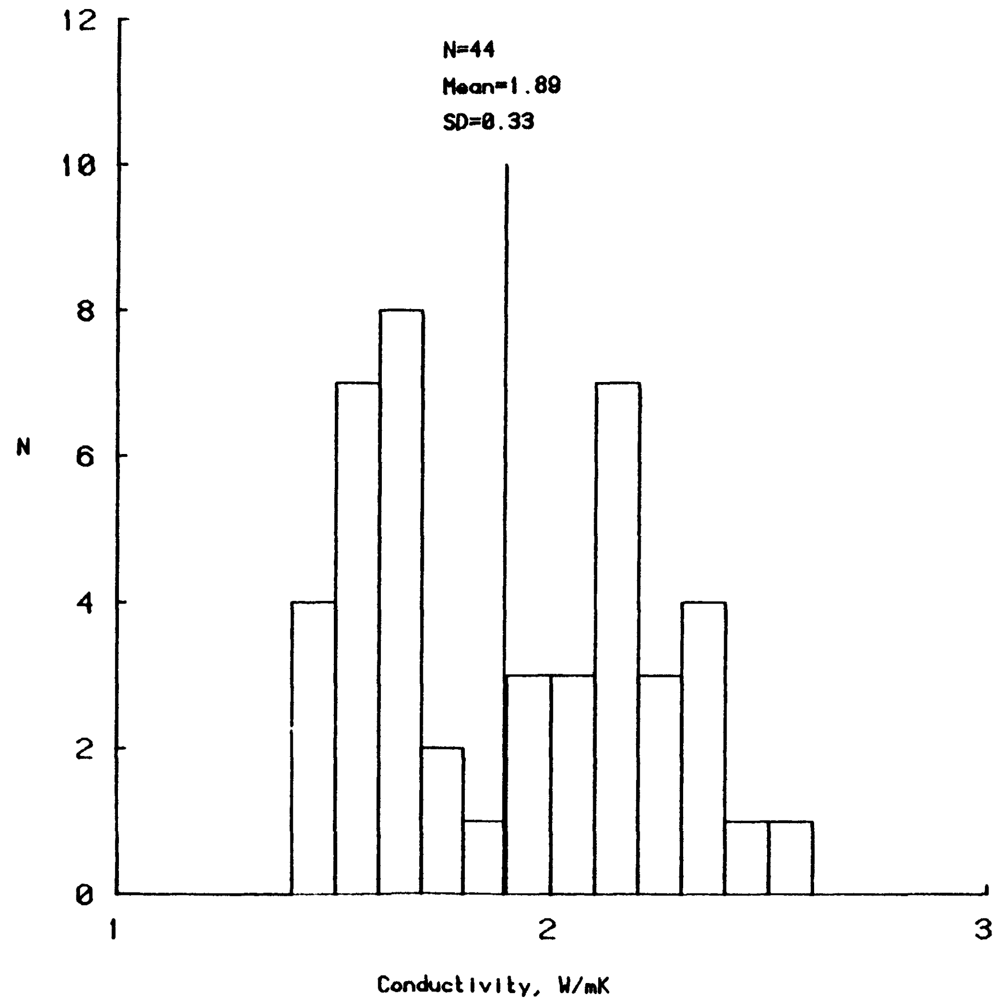

Figure 5. Histogram of in situ thermal conductivities from wells IV03-IV17.

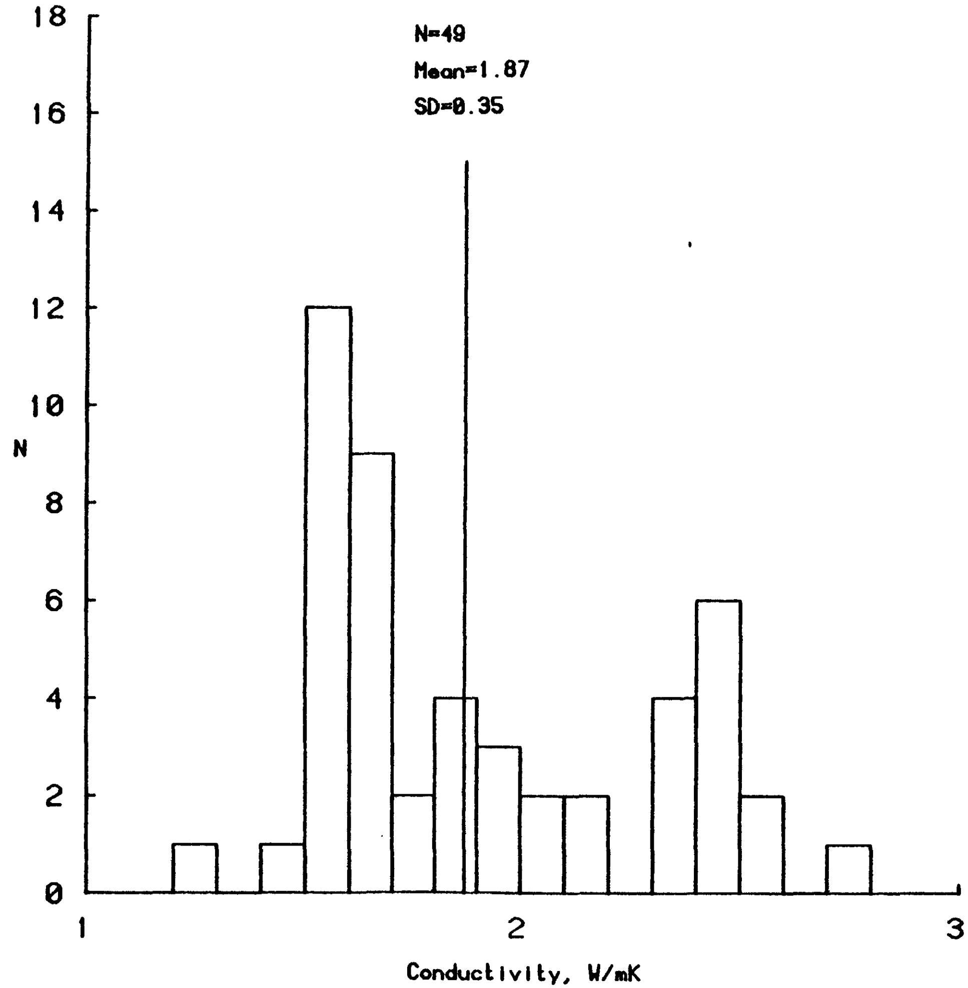

Figure 6. Histogram of in situ thermal conductivities from the Glamis - East Brawley area (see Mase and others, 1981).

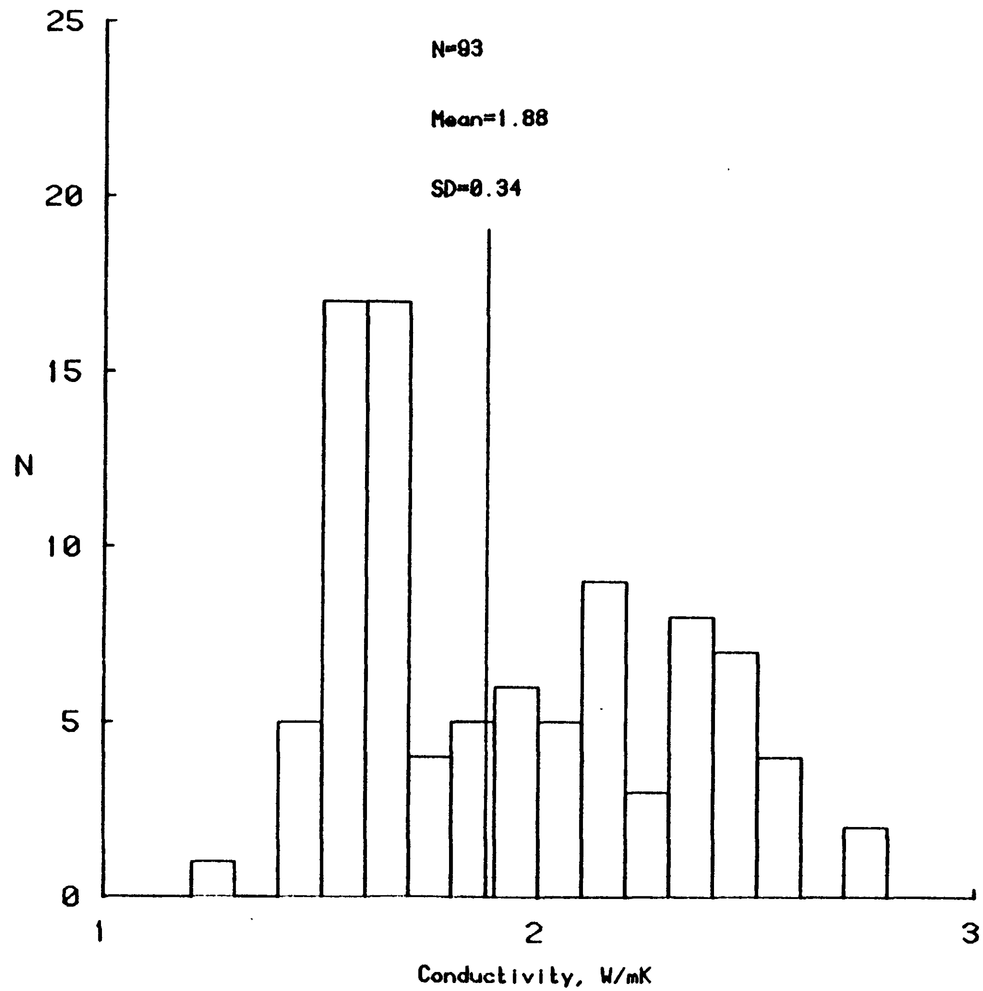

Figure 7. Histogram combining the conductivity data from wells IV03-IV17 and the Glamis - East Brawley area (Figures 5 and 6).

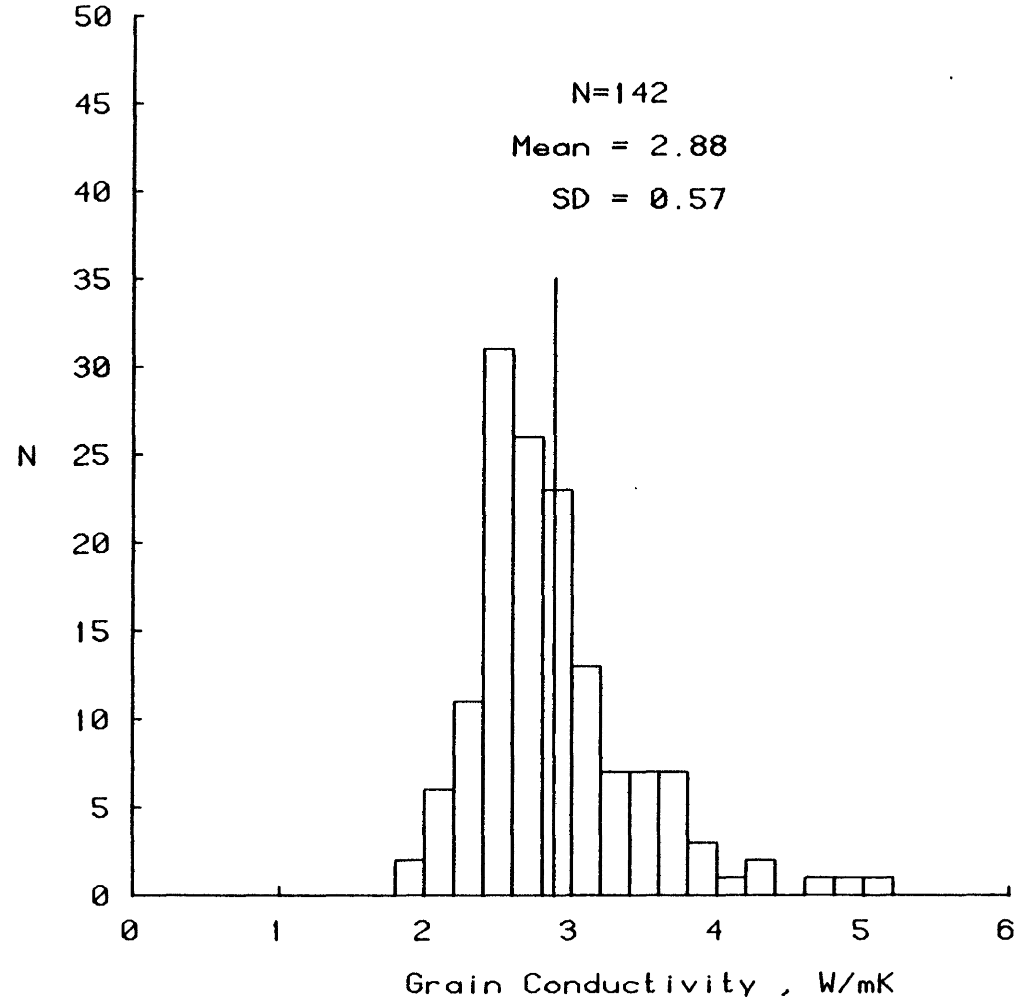

Figure 8. Grain thermal conductivities measured on drill cuttings from wells IV03-IV17.

TABLE 1. In situ thermal conductivities, Western and Central Imperial Valley

Well #	Depth m	K $Wm^{-1} K^{-1}$	Mean	S.D.	Well #	Depth m	K $Wm^{-1} K^{-1}$	Mean	S.D.
IV03	61	1.52			IV14	61	2.20		
		1.51				93	2.19		
							2.18		
			1.52	--		121	1.94		
							1.71		
IV05	66	2.31						2.04	0.22
	134	1.83							
					IV15	66	2.32		
			2.07	--		98	1.64		
							1.70		
						125	2.34		
IV10	66	2.25					2.41		
		2.18						2.08	0.38
		2.17							
	139	1.47			IV16	61	1.62		
			2.02	0.37			1.52		
						88	1.61		
IV11	61	1.45					1.61		
		1.44				107	2.36		
	125	2.08					2.55		
	139	2.01						1.88	0.45
			1.75	0.35					
IV12	66	1.44			IV17	61	1.58		
	93	1.99					1.54		
		2.18					1.54		
	130	2.26				93	1.68		
		2.27					1.62		
						120	1.62	1.60	0.05
			2.03	0.35					
IV13	61	1.79							
		1.60							
	93	2.08							
		1.91							
	134	2.12							
			1.90	0.21					

All wells: N = 44, K = 1.89, SD = 0.33, SE = 0.05

Glamis: N = 49, K = 1.87, SD = 0.35, SE = 0.05

TABLE 2. Grain Thermal Conductivities for 11 wells in the Western and Central Imperial Valley

Well desig.	Depth m	K $Wm^{-1} K^{-1}$
IV03	27	2.30
	34	2.54
	45	2.89
	54	2.96
	63	2.52
	72	3.98
	82	4.11
	91	3.66
	100	3.64
	104	2.67
	109	2.90
	118	2.98
	127	3.29
	136	3.24
IV04	22	2.65
	31	3.67
	40	3.61
	50	3.17
	59	3.49
	68	3.17
	77	3.54
	86	3.82
	95	3.55
	104	3.78
	114	3.62
	118	3.92
	127	3.51
	136	3.39
IV05	27	3.32
	36	3.37
	45	3.06
	54	3.25
	63	4.35
	72	2.69
	82	2.95
	91	2.92
	100	2.86
	118	3.17
	127	3.70

Well desig.	Depth m	K $Wm^{-1} K^{-1}$
IV10	22	2.80
	31	2.70
	40	2.63
	50	4.79
	59	3.34
	63	3.14
	72	3.07
	82	2.35
	91	2.22
	95	2.30
	100	2.50
	109	3.94
	118	2.54
	123	2.70
	127	2.61
	136	2.40
IV11	27	2.39
	36	2.45
	45	2.22
	54	2.23
	72	1.96
	81	1.98
	95	2.41
	104	2.06
	114	2.72
	123	2.33
	127	2.70
	136	3.04
IV12	27	2.49
	36	2.96
	45	2.66
	54	2.72
	63	2.35
	68	3.00
	77	2.46
	86	2.55
	91	2.96
	95	2.74
	104	3.13
	114	2.63
	123	2.68

TABLE 2. Grain Thermal Conductivities for 11 wells in the Western and Central Imperial Valley (continued)

Well desig.	Depth m	K $Wm^{-1} K^{-1}$
IV13	31	5.13
	40	4.95
	50	2.40
	59	2.86
	63	3.04
	72	2.46
	82	2.58
	91	2.65
	95	2.34
	100	2.41
	104	2.56
	114	2.49
	123	3.41
	132	2.90
IV14	27	2.10
	40	2.76
	50	2.78
	59	4.23
	63	2.90
	72	2.69
	82	2.87
	91	2.75
	95	2.33
	100	2.97
	109	2.86
	117	3.11
IV15	27	2.49
	36	2.17
	45	2.46
	54	2.41
	63	2.46
	68	2.78
	72	2.89
	86	2.60
	95	2.52
	100	2.47
	109	3.47
	123	2.71

Well desig.	Depth m	K $Wm^{-1} K^{-1}$
IV16	31	2.13
	40	2.17
	50	2.55
	54	2.46
	63	2.47
	68	2.04
	77	3.06
	86	2.73
	91	2.91
	95	2.91
	104	2.69
IV17	27	2.54
	36	2.42
	45	2.72
	54	2.48
	59	2.94
	63	2.60
	72	2.58
	82	2.73
	91	3.05
	95	2.44
	104	2.67
	114	2.89
	118	2.98

conductivity (K_s, Table 2) by a geometric mean relation

$$K_f = K_s^{(1-\phi)} K_w^{\phi} \qquad (1)$$

where K_w and ϕ are the thermal conductivity of liquid water and fractional porosity, respectively.

Taking logarithms and rearranging terms in equation 1,

$$\phi = \frac{\ell n\ K_s - \ell n\ K_f}{\ell n\ K_s - \ell n\ K_w} \qquad (2)$$

The 24 values of porosity calculated from equation 2 varied from 8% to 38% (Figure 9) with mean of 26% ± 10% (SD), a value identical to that obtained by Mase and others (1981) for Glamis - East Brawley. If we use the overall means for in situ and grain conductivities (Figures 5 and 8) then from equation 2, ϕ also is 26%. This is some 10% lower than average well-log porosities for the Imperial Valley between 300 and 600 meters. Sediments in the upper ∿200 meters seem to be less permeable than underlying sediments, however, as evidenced by the almost ubiquitous conductive temperature profiles and by the absence of natural discharge of thermal fluids in the Imperial Valley. We may surmise that this is due to more poorly sorted, lower-porosity lacustrine sediments having been deposited in the Imperial Valley during the late Pleistocene and Holocene epochs than previously.

The heat-flow values plotted on Figure 2 for wells IV05-IV17 were calculated by combining interval gradients between successive temperature points with the mean "in situ" thermal conductivity, Table 1, according to

$$q = K \cdot \Gamma \qquad (3)$$

where q is heat flow, K is mean conductivity, and Γ is the interval gradient ($T_{Z2} - T_{Z1}/Z2 - Z1$). We also calculated heat flows more conventionally (Table 3) by using the least-squares temperature gradient and the harmonic mean grain thermal conductivity adjusted according to equation 1 by the mean inferred porosity of 26%. The in situ values tend to be slightly higher than those calculated conventionally (Table 3), but for all wells, the two values agree to well within the estimated uncertainty of the conventional calculation. This agreement is encouraging, even though the two sets of heat-flow determinations are not completely independent.

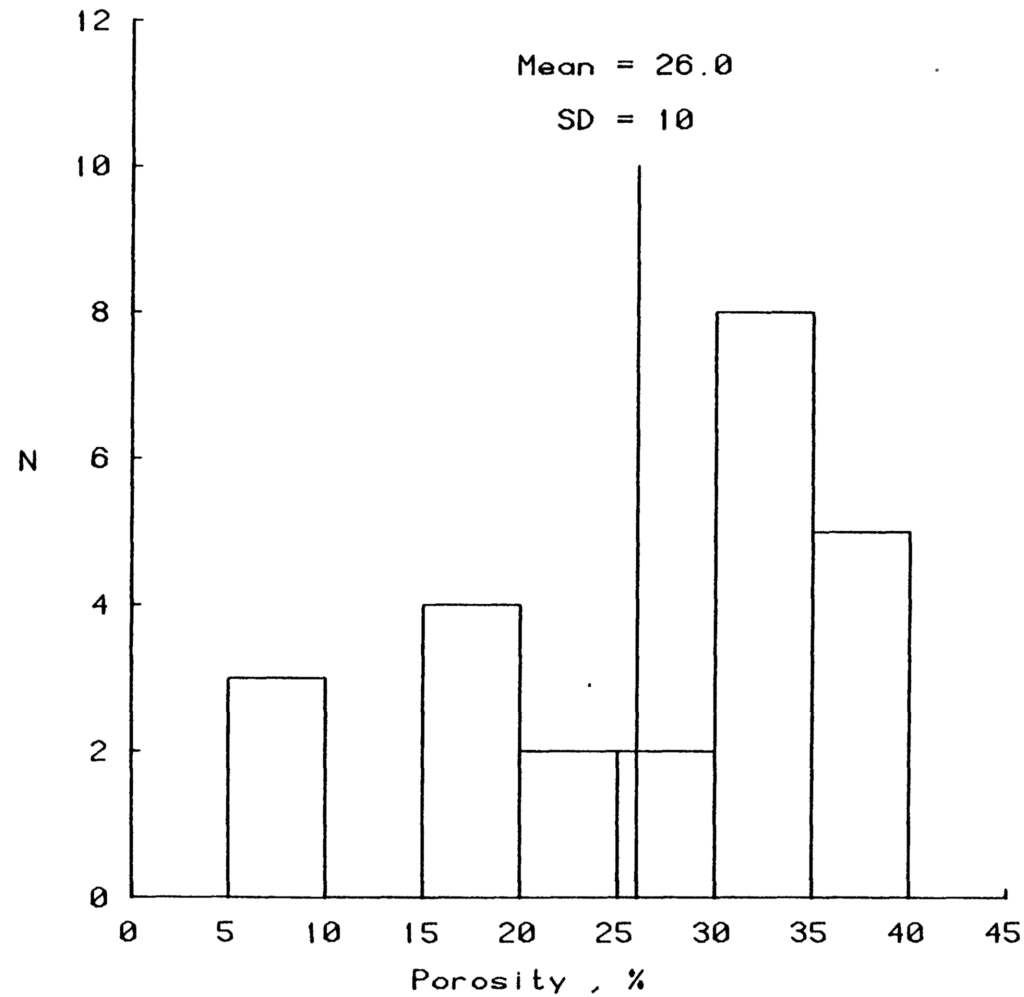

Figure 9. Distribution of porosity estimated from equation 2 based on in situ and grain conductivities measured for the same depths.

TABLE 3. Heat flow calculated conventionally[1] and measured in situ for 11 holes in the Western and Central Imperial Valley

Well designation	Depth interval m	N[2]	Thermal conductivity $W\ m^{-1}\ K^{-1}$		Γ $°C\ km^{-1}$	q, $mW\ m^{-2}$	
			$\langle K_S\rangle$[3]	K_r[4]		$K_R \cdot \Gamma$	In situ
IV03	30-139	14	3.03±0.14	2.0±0.3	38.1±0.1	76±12	---
IV04	67-139	13	3.54±0.06	2.25±0.25	42.5±0.1	96±15	---
IV05	66-134	7	3.16±0.19	2.07±0.3	52.0±0.7	108±17	109
IV10	67-139	11	2.64±0.12	1.81±0.25	47.0±1.0	85±14	88
IV11	61-139	9	2.33±0.12	1.65±0.25	72.0±5.0	119±26	134
IV12	65-130	9	2.70±0.09	1.84±0.25	53.0±5.0	98±22	105
IV13	61-134	11	2.67±0.09	1.84±0.25	66.0±1.8	120±20	130
IV14	61-121	9	2.90±0.14	1.94±0.3	43.0±2.0	83±17	92
IV15	66-125	8	2.71±0.10	1.84±0.25	67.6±2.2	124±21	142
IV16	61-107	7	2.64±0.15	1.81±0.25	49.0±0.5	89±13	92
IV17	62-120	8	2.73±0.07	1.85±0.25	27.8±0.8	51±8	46

[1]Calculated from least-squares gradient and harmonic mean grain conductivity corrected for 26% porosity.

[2]Number of conductivity measurements.

[3]$\langle K_S\rangle$ = Harmonic mean grain conductivity.

[4]$K_r = \langle K_S\rangle^{(1-\phi)} \cdot K_w^{\phi}$, K_w = Thermal conductivity of water, ϕ = fractional porosity.

GENERAL APPLICABILITY OF REGIONAL MEAN IN SITU THERMAL CONDUCTIVITY

The agreement between mean porosities inferred from in situ and grain conductivities over an area encompassing IV03 through 17 and the Glamis - East Brawley measurements (unlabeled circles, Figure 2) is encouraging, and leads to the question of whether our mean in situ thermal conductivity of 1.88 ± 0.34 (SD) $W\ m^{-1}\ K^{-1}$ (Figure 7) might be generally applicable to the sediments in the upper ~100-200 meters of the Imperial Valley. On the one hand, the fact that the mean (Figure 7) falls within a part of the histogram representing only a few actual determinations is somewhat discouraging; on the other hand, the stratification of sediments in most wells reflects this bimodality with layers composed primarily of sand and silt alternating with relatively clay-rich layers, although layers composed purely or even primarily of clay are relatively rare (R. W. Rex, personal communication, 1983). C. A. Swanberg (personal communication, 1984, and manuscript in preparation) has pointed out that for alluvial material, bimodal distributions of conductivity will result from identical lithologies from measurements taken above and below the water table. The natural water table in the Imperial Valley is quite shallow (usually <30 m), and we made our first downhole probe run at 60 m or deeper. Thus, we prefer the explanation of alternating clay-rich and sand-rich layers.

If we examine the heat-flow data in Table 3, we may note that in all but two instances (IV04 and IV11) using the mean conductivity rather than that specific to the site in question would characterize the heat flow to within ±10%. For IV11 we would be within 13%, and IV04 was a special case insofar as the sediments were very arenaceous and sufficiently well cemented that we could not penetrate the formation more than 2-3 cm with the downhole heat-flow probe. A similar result would be obtained in the Glamis - East Brawley area (cf., Table 2, Mase and others, 1981).

We thus conclude that, for the depth range 30-150 m (60-150 m in areas that have been irrigated for a significant period (see Mase and others, 1981), we may combine the average thermal gradient from any well with our mean in situ thermal conductivity (equation 3) and obtain a reliable estimate of heat flow in the majority of cases.

HEAT-FLOW ESTIMATES FROM INDUSTRY DATA

R. W. Rex (personal communication, 1983) made available temperature-gradient data from 260 wells deeper than 60 m (dots, Figure 2). Based on the apparent generality of our mean thermal conductivity, we combined the gradient data with the mean conductivity of 1.88 $Wm^{-1} K^{-1}$ (equation 3) to obtain estimates of heat flow. Where Republic's data (dots) overlap with ours (open circles), the agreement is, in general, very good (Figure 2) lending further credence to our assumption regarding the general applicability of our conductivity value. The distribution of heat-flow data is treated in detail in the discussion. For the present, we note, (Figure 2) that most heat flows are in the range 100-200 mW m^{-2}, with higher values concentrated in known geothermal fields (cf., Figure 1).

RE-EVALUATION OF EAST MESA DATA

Swanberg (1974a, 1974b, 1975) updated some earlier estimates of heat flow from the East Mesa area by Combs (1971, 1972) and presented additional data for the area. In the absence of detailed information on thermal conductivity, Swanberg (1974a) devised an ingenious method of estimating heat flow based on the temperature gradients within the "best clay," a layer greater than 3 m thick of low thermal conductivity having a characteristic signature on passive γ-ray logs, and characterized by the highest interval temperature gradients on the temperature logs. By plotting temperature gradients as a function of heat flow from four wells in which there was sufficient conductivity data to specify heat flow, he inferred a thermal conductivity (from the slope of the q-Γ line, see equation 3) of 1.0 W m^{-1} K^{-1} for the "best clay," and applied this to the "best clay" layers in other wells in the area.

To bring the East Mesa data into conformity with our other heat-flow estimates, we used our mean thermal conductivities to calculate heat flow within the lowermost linear segment of each temperature profile (Table 4). Some of Swanberg's values were higher than ours, but in general, our heat-flow estimates were significantly higher than his. For 28 sites, our mean heat flow (242 mW m^{-2} ± 19 SD) is some 20% higher than the mean of Swanberg's (1974a) values, 193 ± 13 (SD).

We believe that the discrepancy arises from Swanberg's (1974a) use of unrepresentative or erroneous values of thermal conductivity (Combs, 1972) or from the fact that some of the "best clay" intervals probably contained some sand and silt and thus, had higher conductivities than the 1.0 Wm^{-1} K^{-1} assumed by Swanberg. We, therefore, prefer our own estimates to the previously published ones.

TABLE 4. Re-evaluation of some East Mesa heat flows using a constant thermal conductivity of 1.88 W m^{-1} K^{-1}

USBR well #	Depth range (meters)	Γ °C/km	q mW m^{-2}	USGS cross reference	Published q
77	46- 55	144	271	SW21	159
78	70- 76	123	231		
79	46- 73	87.7	165	SW15	264
80	49- 78	83.6	157	SW14	151
81	50- 76	76.3	143	SW13	159
82	58- 75	69.7	131	SW10	126
83	46- 77	124	233	SW	209-
122	46-171	182	343	SW32	230
123	46-171	201	378	SW34	272
127	46-152	164	308	SW24	184
128	46-137	152	285	SW28	230
129	46-152	144	271	SW31	239
201	76-152	105	197	SW46	142
202	46-146	180	339	SW45	214
203	46-143	153	287	SW43	214
204	58-122	189	355	SW39	331
205	58- 91	209	393	SW38	276
206	116-152	164	308	SW30	268
207	76-152	100	189	SW17	209
208	82-134	102	193	SW	250-
209	134-152	86	162	SW	250-
210	46- 76	186	349	SW37	247
211	46- 99	208	390	SW36	239
212	46- 95	202	380	SW29	226
213	46-125	123	232	SW23	180
214	61-101	68.1	128	SW22	88
215	46- 98	72.2	136	SW18	113
216	91-131	69.5	131	SW12	109
217	67-128	60.4	113	SW11	134
218	79- 95	150	282	SW	300-
219	83-158	66.8	126	SW	170-
221	46-152	27.9	52	SW20	63
222	61-104	76.3	143	SW16	113
223	122-183	102	192	SW26	226
224	46-82	197	370	?	?

HEAT-FLOW ESTIMATES FROM TWO DEEP TEST WELLS

"Direct use" wells were drilled at the Holly Sugar plant near Imperial (HOLL) and on the east side of El Centro (ELCT) (Figure 2). The wells were 1.8 and 2.5 km deep, respectively (Figure 10). The log in the Holly Sugar well was obtained by us more than six months after drilling, and thus should represent an equilibrium temperature profile. The temperature log in the El Centro well (Figure 10) was made by a commercial well-logging firm only 16 days after completion of a 37-day drilling period. Near-surface temperatures indicate considerable disequilibrium as we would expect a surface temperature in the 24 to 27 °C range in contrast to the 30+ °C observed. The "stairsteps" in the El Centro log represent depths where the temperature sonde was stopped (every 500 feet or ∿150 m) to allow sonde and well fluid to equilibrate (logging speed was ∿10 m/min).

No lithologic information or samples were available from the Holly Sugar well. Hence, the only heat-flow estimate we could make was by combining the gradient in the upper ∿150 m with our regional average conductivity of 1.88 W m^{-1} K^{-1}. Much curvature is evident in the upper 200 m of the HOLL profile (Figure 11), but there is a relatively linear segment between 80 and 160 m -- the depth interval used to establish the regional mean conductivity. The least-squares temperature gradient over this interval is 49.5 ± 0.2 °C km^{-1} which when combined with our regional mean conductivity yields a heat flow of 92 mW m^{-2}. The temperature gradient increases sharply below 300 m (Figure 10) then decreases gradually, consistent with a more-or-less constant grain conductivity and the decrease in porosity generally observed between 300 and 2500 meters in the Imperial Valley (Rex and others, 1971). The least-squares temperature gradient between 300 and 1500 m is 66.5 ± 0.1 °C/km. If the heat flow at depth is 92 mW m^{-2} as we have estimated for the upper ∿160 m, then the mean conductivity is 1.38 W m^{-1} K^{-1}. For a grain conductivity of 2.9 W m^{-1} K^{-1} (consistent with our results from the upper ∿150 m of the Valley, Figure 8), a mean porosity of ∿45% in the interval 300 to 1500 m is required to produce this formation conductivity. If mean porosity is lower, then so is the grain conductivity. Alternatively, if the gradient is disturbed or the regional average conductivity above 160 m is not applicable to this well, then the heat flow may be higher than our estimate of 92 mW m^{-2}. (If we use conductivities from the same depths from the El Centro well, discussed below, the mean heat flow between 300 and 1800 m is 113 mW m^{-2}.) In the absence of deep information on porosity and conductivity from this well, however, we cannot choose among the various alternatives, and we adopt the value of 92 mW m^{-2} as our "best estimate" for this site, even though it may be an underestimate.

For the El Centro site, both drill cuttings and numerous geophysical logs were available, and we were able to estimate the formation thermal conductivities in a variety of ways (Table 5). The pertinent basic data were the porosity (ϕ) from density logs, the interval compressional wave velocity (v_p), and the grain thermal conductivity (K_s) measured on drill cuttings.

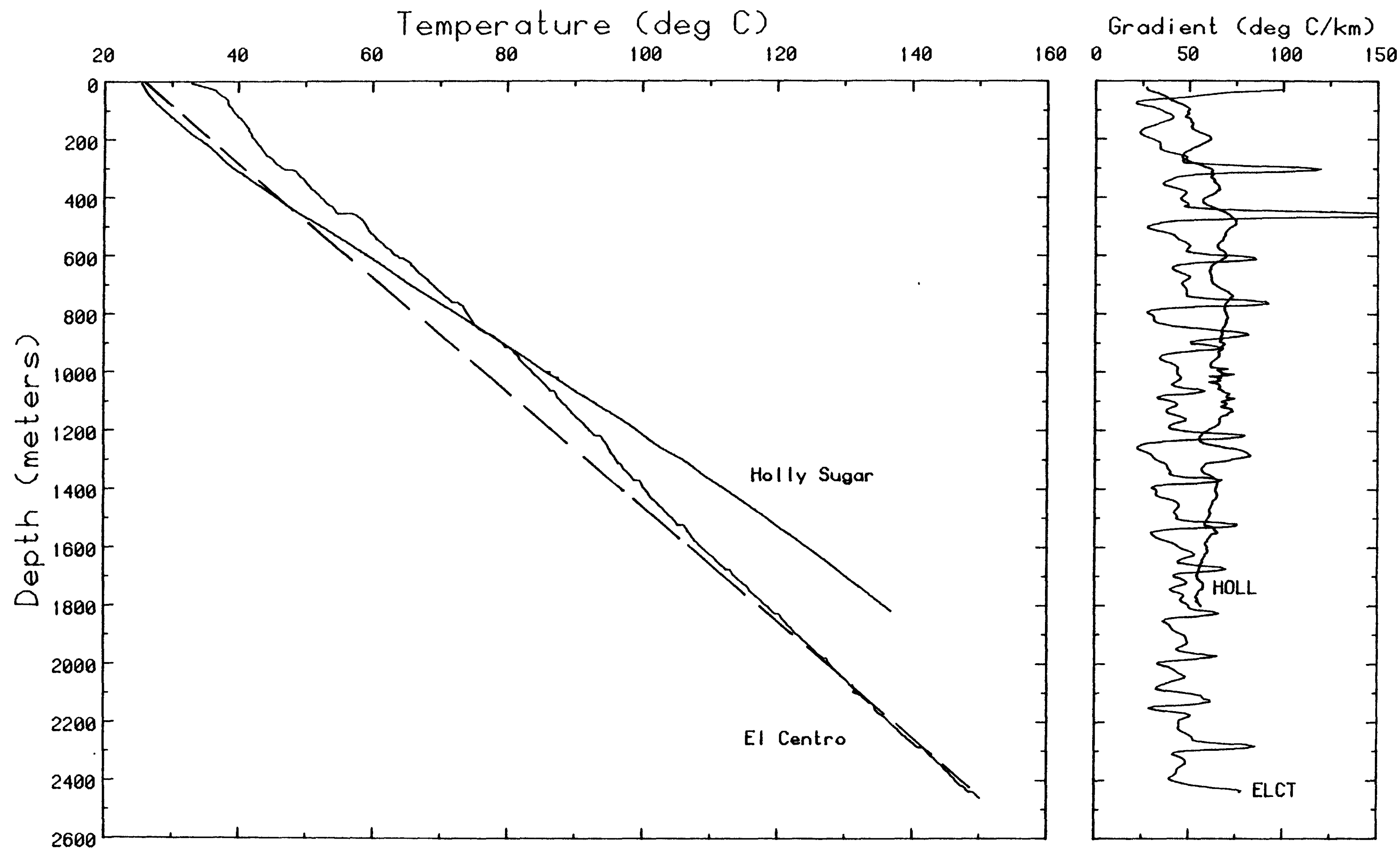

Figure 10. Temperature and gradient profiles for ELCT and HOLL (Figure 2). Dashed straight line connects an assumed surface temperature of 25°C to the bottom-hole temperature for ELCT.

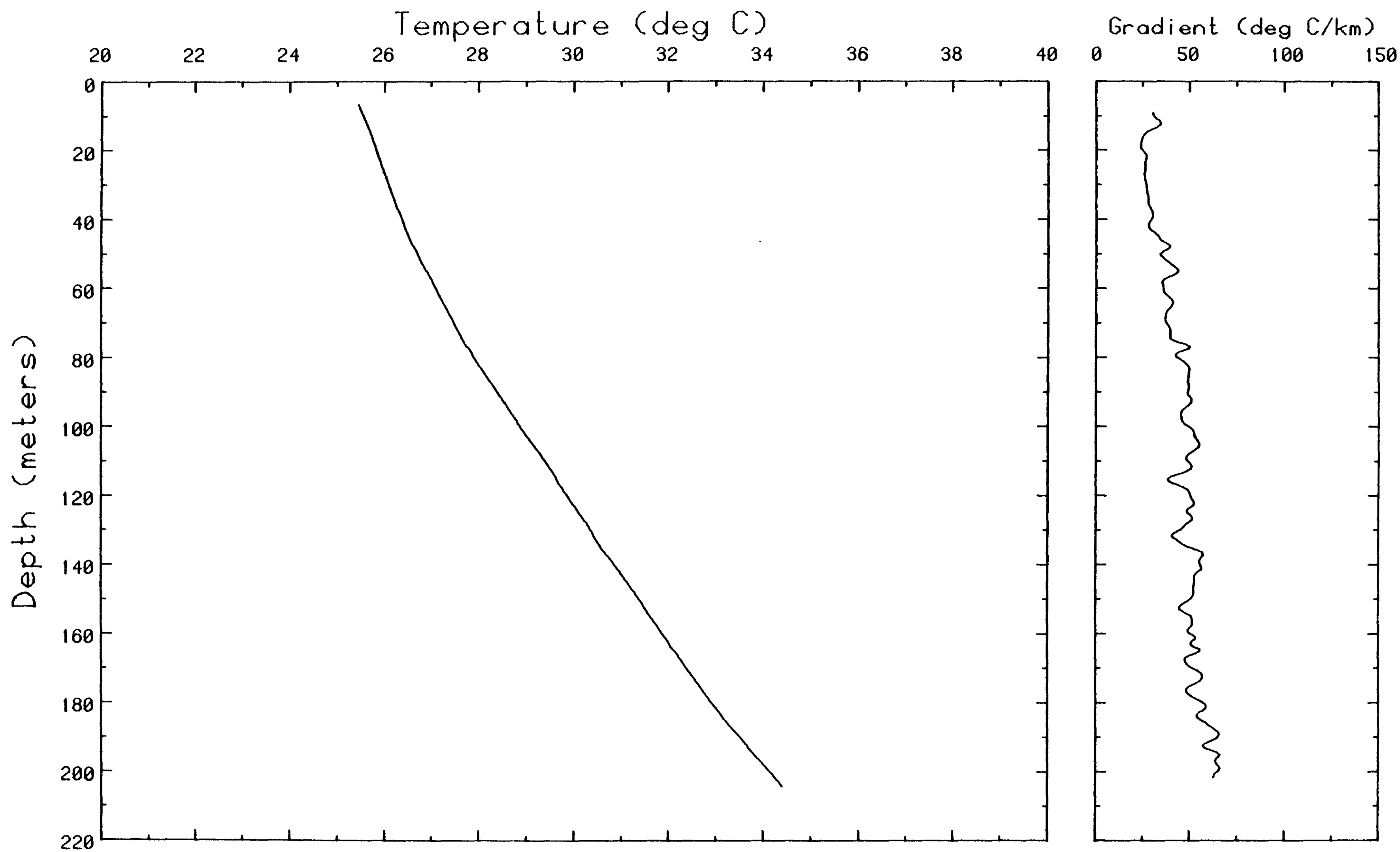

Figure 11. Temperature and gradient profiles for the upper 200 m of the Holly Sugar well.

TABLE 5. Porosity (PHI) and compressional wave velocity (V_p) from geophysical logs, grain conductivity (K_s) and model conductivities (K1 through K5) for El Centro well.

Z m	PHI %	Vp km/s	Ks	K1	K2	K3	K4	K5
			W/mK					
312	40	1.75	2.03	1.28	1.00	0.46	1.30	1.20
367	40	1.85	2.55	1.47	1.09	0.53	1.36	1.24
422	33	2.00	2.55	1.62	1.23	0.91	1.46	1.52
477	30	2.00	2.62	1.73	1.23	1.03	1.46	1.62
532	33	1.85	2.75	1.71	1.09	0.81	1.36	1.47
587	30	2.05	2.20	1.53	1.28	1.07	1.50	1.63
614	35	2.10	2.48	1.56	1.32	0.90	1.53	1.49
642	30	2.20	2.24	1.55	1.41	1.17	1.60	1.68
696	35	2.20	2.42	1.54	1.41	0.97	1.60	1.52
751	36	2.10	2.92	1.71	1.32	0.86	1.53	1.45
806	26	2.30	2.48	1.76	1.50	1.40	1.66	1.85
861	35	2.10	2.47	1.56	1.32	0.90	1.53	1.49
916	32	2.40	2.51	1.64	1.60	1.23	1.73	1.69
971	25	2.40	2.65	1.88	1.60	1.51	1.73	1.92
1026	35	2.40	2.60	1.62	1.60	1.11	1.73	1.59
1081	33	2.60	2.63	1.68	1.78	1.33	1.86	1.72
1135	23	2.30	2.15	1.65	1.50	1.52	1.66	1.95
1190	33	2.80	3.17	1.90	1.96	1.47	2.00	1.79
1245	26	2.80	3.82	2.44	1.96	1.75	2.00	2.02
1300	28	2.60	2.44	1.70	1.78	1.53	1.86	1.88
1355	25	2.80	3.43	2.29	1.96	1.79	2.00	2.05
1410	28	2.70	2.42	1.70	1.87	1.60	1.93	1.92
1465	33	2.60	2.62	1.68	1.78	1.33	1.86	1.72
1519	35	2.80	2.21	1.46	1.96	1.39	2.00	1.72
1574	25	2.80	3.52	2.33	1.96	1.79	2.00	2.05
1629	28	3.00	2.23	1.60	2.14	1.81	2.13	2.02
1684	31	2.90	2.55	1.69	2.05	1.62	2.06	1.89
1747	27	3.00	2.85	1.94	2.14	1.85	2.13	2.05
1807	31	3.00	2.62	1.73	2.14	1.69	2.13	1.92
1868	28	2.80	2.55	1.76	1.96	1.67	2.00	1.95
1929	23	3.60	3.48	2.39	2.69	2.42	2.53	2.38
1990	25	3.50	3.04	2.09	2.60	2.27	2.47	2.28
2051	25	3.20	3.90	2.52	2.33	2.07	2.27	2.18
2112	22	3.30	2.94	2.13	2.42	2.26	2.33	2.32
2173	17	3.70	2.37	1.92	2.78	2.73	2.60	2.61
2234	12	3.70	3.03	2.53	2.78	2.93	2.60	2.78
2295	19	3.80	4.67	3.24	2.87	2.72	2.67	2.58
2356	16	3.80	5.05	3.66	2.87	2.84	2.67	2.68
2417	13	3.80	3.36	2.73	2.87	2.96	2.67	2.78
2478	12	3.60	3.84	3.12	2.69	2.86	2.53	2.75

From these parameters, the most reliable estimate of formation thermal conductivity was K1 which was calculated from (cf., equation 1)

$$K1 = K_s^{1-\phi/100} \cdot K_w^{\phi/100} \quad (4)$$

where ϕ in this case is the % porosity (PHI, Table 5).

As an exercise, we compared K1 and conductivity estimates made from two of the relations established by Goss and Combs (1975) from measurements on core specimens from the Imperial Valley. The relations tested were

$$K2\ (W\ m^{-1}\ K^{-1}) = -0.595 + 0.913\ V_p\ (Km\ s^{-1}) \quad (5)$$

and

$$K3 = 0.842 - 0.04\phi + 0.695\ V_p \quad (6)$$

Below 1 km (Tables 5 and 6, Figure 12), K2 and K1 are in reasonable agreement and below 1.5 km both equations 5 and 6 yield conductivity estimates consistent with the "measured" values (K1). Above 1 km (Figure 12, Table 6), it is clear that the Goss-Combs relations do not adequately predict the formation conductivity. Examination of their basic data showed that Goss and Combs (1975) had no core data from the Imperial Valley at the low conductivity - low velocity end of the scale.

As a further exercise, we performed linear regression analyses on our own basic data and derived the following relations for the data set of Table 5:

$$K4 = 0.124 + 0.669\ V_p \quad (7)$$

and

$$K5 = 1.94 - 0.033\phi + 0.334\ V_p \quad (8)$$

These relations provide a better overall fit to our "reliable" estimate (K1) of formation conductivity (Figure 13) than the original Goss-Combs relation, although not as good a fit at the high-conductivity end (Table 6, 1.5 to 2.5 km).

We may reasonably expect that equations 7 and 8 will provide reliable estimates of thermal conductivity for other wells in the Imperial Valley for which cuttings samples are not available but for which velocity and porosity logs are.

Initially, we made heat-flow estimates between 305 and 2500 m at 305 m intervals by combining least-squares gradients from the observed temperature profile (Figure 10) with harmonic mean values of K1 (Table 5) over the same intervals. The interval heat flows were inconsistent; decreasing monotonically from 84 mW m^{-2} in the interval 305 to 610 m, to 71 between 1220

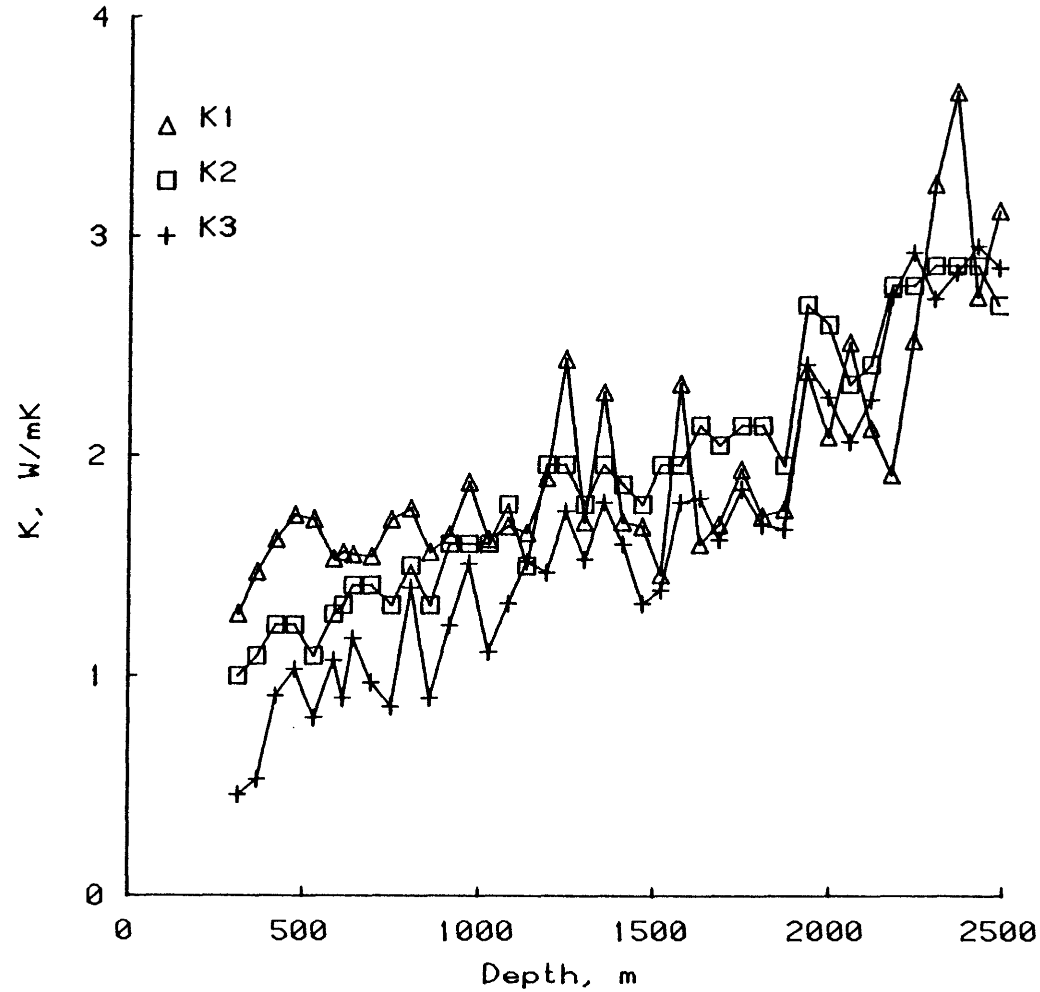

Figure 12. Geometric mean conductivity K1 and conductivities estimated from the Goss-Combs relations (K2 and K3) as a function of depth in the El Centro well.

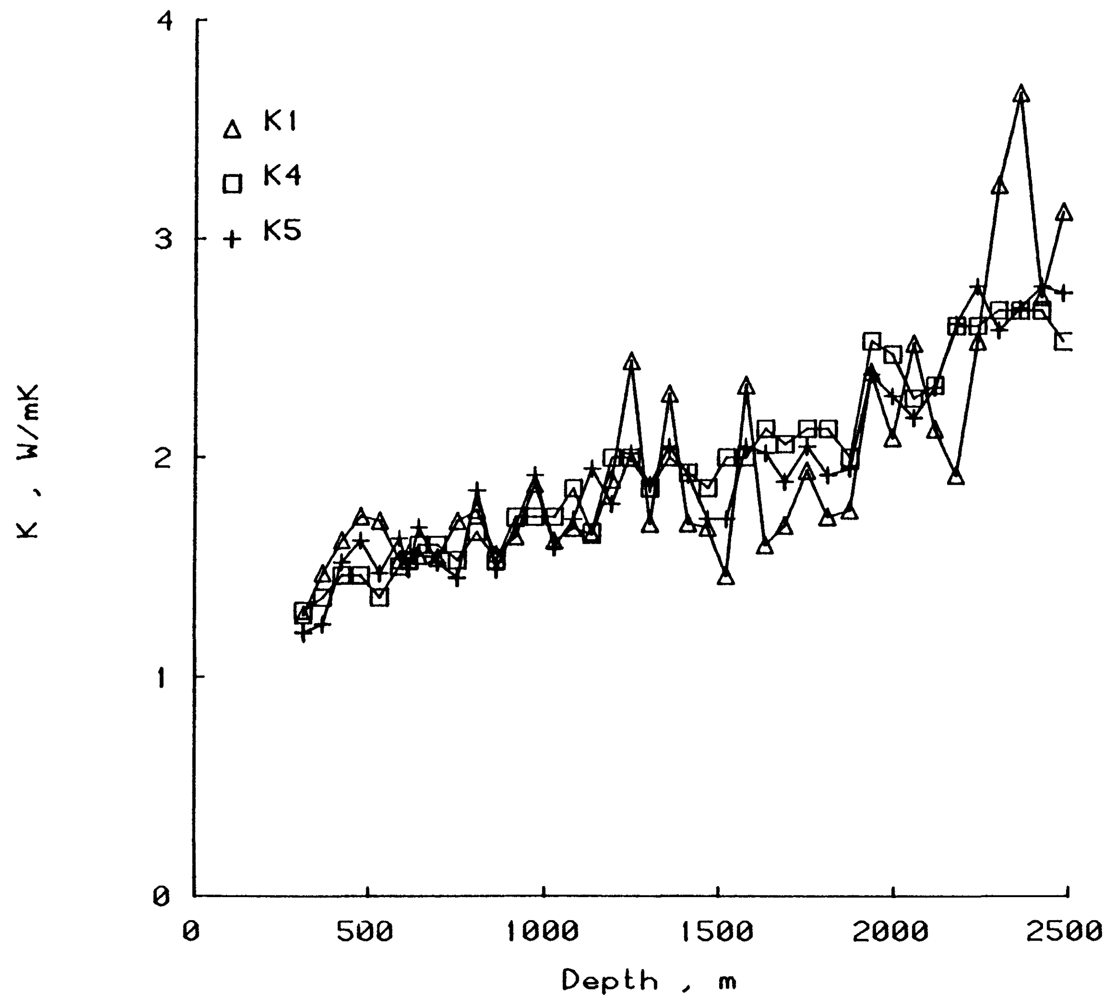

Figure 13. Geometric mean conductivity, K1, and conductivities estimated from the modified Goss-Combs relations (K4 and K5) as a function of depth in the El Centrol well.

TABLE 6. Comparison of average thermal conductivity estimates made from cuttings and well-log porosities (K1), from the Goss-Combs relations (K2 and K3) and from the modified Goss-Combs relations (K4 and K5), El Centro well

Depth range	N	K1 (SD)	K2 (SD)	K3 (SD)	K4 (SD)	K5 (SD)
300-500	4	1.52 (0.20)	1.14 (0.11)	0.73 (0.28)	1.40 (0.08)	1.40 (0.10)
500-1000	10	1.64 (0.12)	1.38 (0.16)	1.08 (0.24)	1.58 (0.11)	1.62 (0.17)
1000-1500	9	1.85 (0.30)	1.80 (0.16)	1.49 (0.21)	1.88 (0.12)	1.85 (0.15)
1500-2000	9	1.89 (0.32)	2.18 (0.27)	1.83 (0.32)	2.16 (0.20)	2.03 (0.20)
2000-2500	8	2.73 (0.58)	2.70 (0.21)	2.67 (0.33)	2.54 (0.16)	2.59 (0.22)

and 1520 m then increasing to 133 mW m^{-2} in the lowermost 300 m. We attributed these inconsistencies to the obvious disequilibrium in temperatures. Since the lowermost part of the temperature profile should be very nearly in equilibrium, the equilibrium mean surface temperature is around 25°C and the thermal conductivity structure of the well is adequately characterized by K1 (Table 5), we elected to estimate heat flow based on the product of the harmonic mean K1 and the mean gradient between the assumed surface temperature of 25°C and the bottom-hole temperature, represented by the dashed straight line of Figure 10. The mean gradient is 50.85 °C/km and the harmonic mean of 39 values of K1, 1.83 ± 0.06 (SE) W m^{-1} K^{-1}, resulting in a heat flow of 93 mW m^{-2}.

As a test of our assumptions, we constructed a synthetic temperature profile (Figure 14) constrained by the heat flow of 93 mW m^{-2}, a surface temperature of 25°C, and the conductivity structure as characterized by K1 (Table 5). Qualitatively, the synthetic profile is very plausible, indicating elevated temperatures in the upper half of the observed profile, and depressed temperatures in all but the lowermost portion of the lower half. The fit between the two profiles near the bottom of the hole could be improved by a combination of a slightly higher surface temperature and slightly lower conductivity in the upper 300 m (we assumed a value of 1.88 W m^{-1} K^{-1}, our regional average from shallow holes).

Although somewhat uncertain, our heat-flow estimates from two deep wells confirm that the thermal regime of the upper ~2.5 km is conductive over much of the Imperial Valley (an observation made independently by others in several exploratory wells) and indicate that the heat flows obtained at relatively shallow depths (<200 m) are representative of the deeper thermal regime (Figure 2).

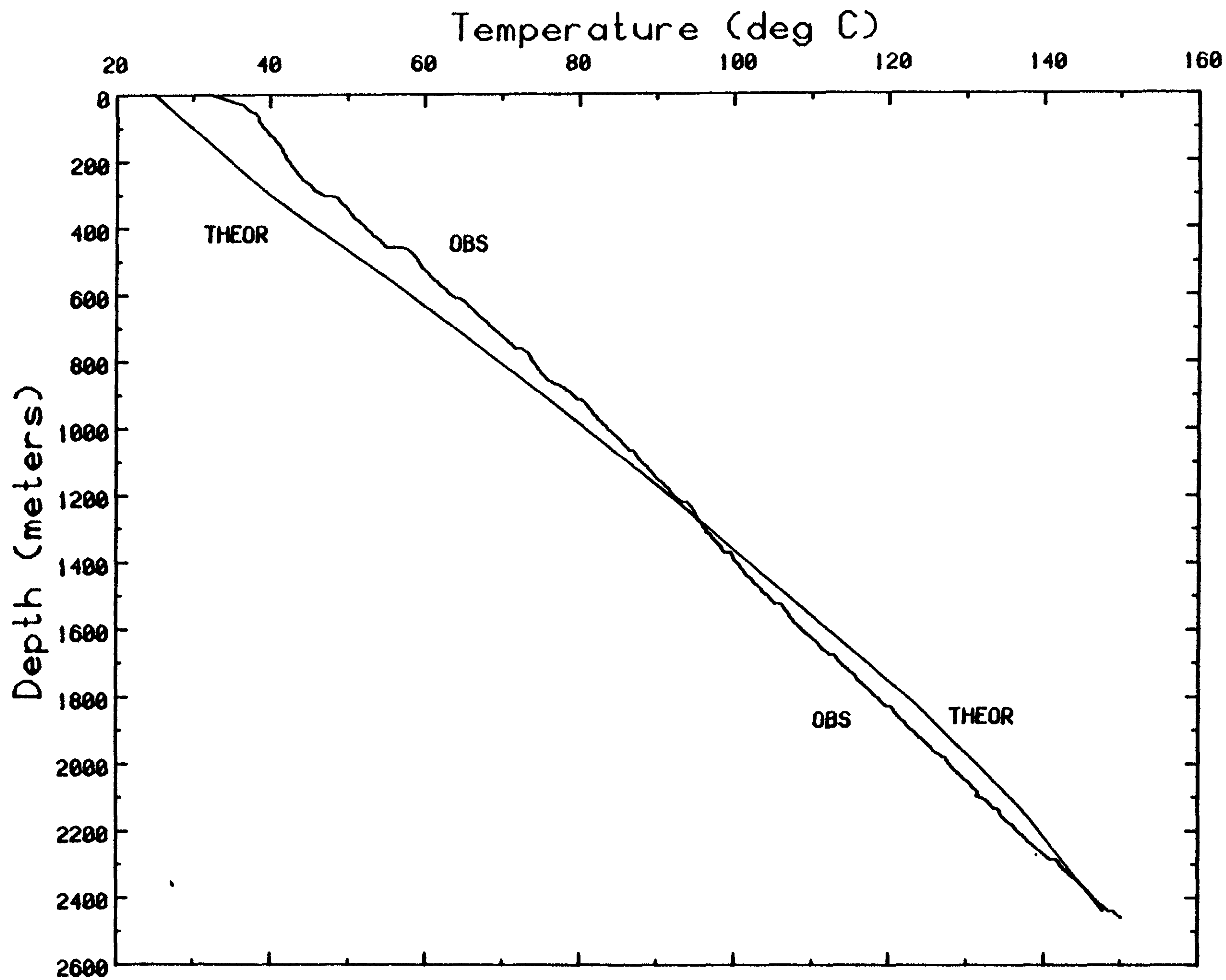

Figure 14. Temperature profiles for the El Centro well. "OBS" is the observed disequilibrium profile; "THEOR", the equilibrium profile calculated from the observed thermal conductivity structure, a surface temperature of 25°C and a heat flow of 93 mW m^{-2}.

DISCUSSION

We now have 322 estimates of heat flow from the unconsolidated deltaic and lacustrine sediments of the Imperial Valley to varying depths (although most wells are shallower than 160 m) and of variable quality. The density of coverage varies (Figure 2) even though we have sampled most parts of the valley. Based on sparse coverage, the western edge of the valley appears to have generally lower heat flows than the remainder, either from lateral recharge or from the lack of heat sources at depth. Within the overall high heat-flow pattern, there are clusters of very high heat flow generally associated with known geothermal areas (cf., Figures 1 and 2) flanked by zones of relatively lower heat flow. Inasmuch as there is no natural discharge of thermal fluids within the Imperial Valley, we interpret these variations in terms of local convective upwellings and corresponding downward limbs in the relatively permeable sediments. Based on observations in fairly deep wells (e.g., Figure 10) the convective systems appear to be fairly deep (∿2 km or greater) in some localities, although they come much closer to the surface at other sites.

The primary purpose of the present study was to provide a heat-flow constraint on physical and thermal models for the Salton Trough (Lachenbruch and others, 1983a, 1983b, 1984). Because of the variability both in heat flow and distribution of values, a simple average of all heat flows would not be satisfactory for this purpose. To take account of the uneven distribution, we divided the valley into 3' × 3' areas (approximately 5 km on a side), averaged all heat flows within each such element (Figure 15), then averaged these mean values to obtain our characteristic heat flow for the Imperial Valley. The resulting distribution of 99 3' × 3' elements (Figure 16) has a strong mode at ∿140 mW m^{-2}, but because of very high averages from some of the known geothermal areas (Salton Sea, Brawley and Heber, Figure 1), the distribution is somewhat skewed with a mean of 166 mW m^{-2}. If we exclude elements whose average heat flow is >280 mW m^{-2} (crosshatched, Figure 16), which are almost certainly over-represented in the entire population, we are left with 89 elements demonstrating a more normal distribution with mean of ∿140 mW m^{-2}, a value which we adopt as our surface heat-flow constraint.

The surface heat flow is the sum of the mantle and lower crustal components and the heat produced in the valley sediments themselves. It is convenient, when modeling fundamental tectonic processes on the continents, to subtract the upper crustal component to arrive at a "reduced heat flow." Since the Colorado River Delta sediments found in the Imperial Valley were derived, in large part, from granitic crystalline rocks, we might expect a sizable component of the observed background heat flux to come from radioactive decay within these rocks.

A composite one-kilogram sample from each of the Glamis wells (Mase and others, 1981) and from wells IV03 through IV17 was analyzed by γ-ray spectrometry for U, Th, and K (A. R. Smith, personal communication, 1983, 1984). The results and the resulting radiogenic heat-production values (Table 7) are in the range one would expect from granitic detritus. The mean of 21 values is 1.45 μW m^{-3} ± 0.29 SD. Using an average thickness of 10 km for the sediments (see Lachenbruch and others, 1984), the reduced heat flow will then be about 125 mW m^{-2}.

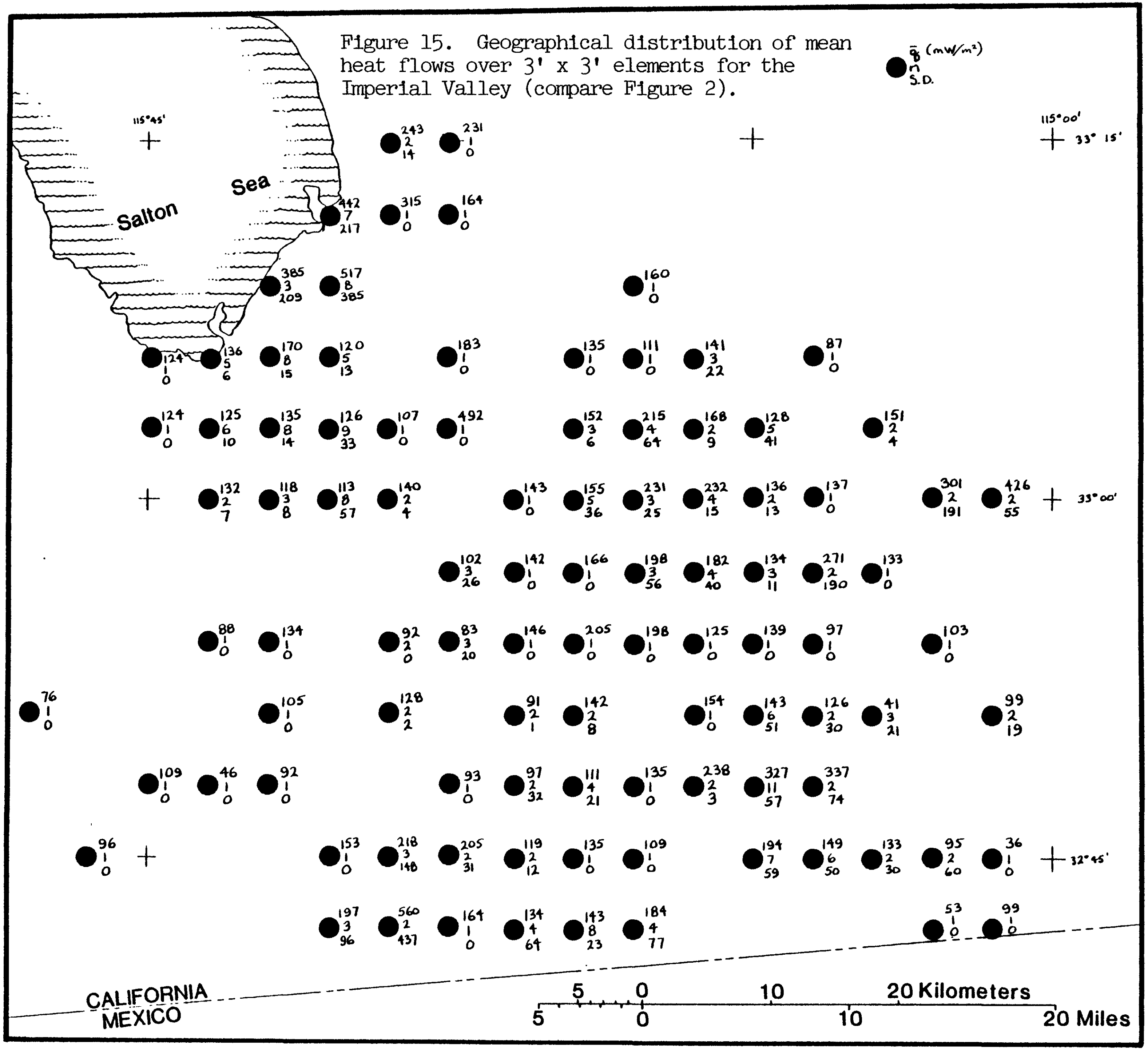

Figure 15. Geographical distribution of mean heat flows over 3' x 3' elements for the Imperial Valley (compare Figure 2).

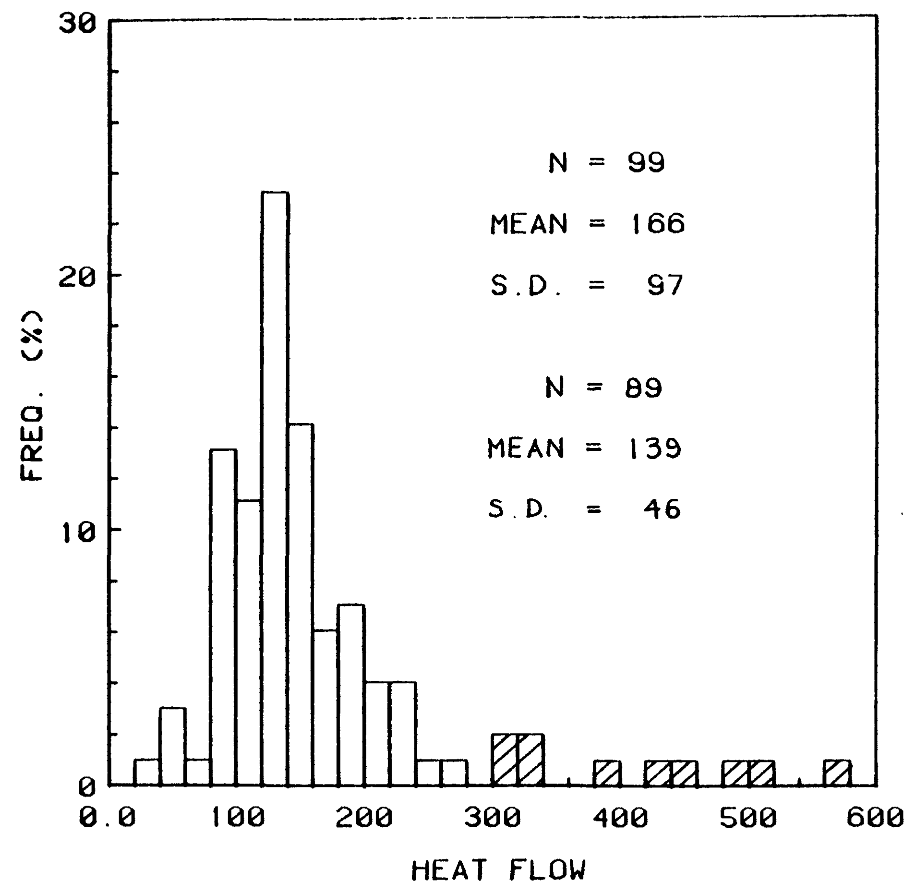

Figure 16. Distribution of 3' x 3' mean heat flows within the Imperial Valley.
Heat flows greater than 280 mW m^{-2} (crosshatched) were excluded from the lower mean.

TABLE 7. Radiogenic heat production of Imperial Valley sediments

Well	U ppm	Th ppm	K %	Th/U	ρ[1]	A $\mu W\ m^{-3}$
GL03	2.54	8.66	2.23	3.41	2.65	1.48
GL10	2.18	8.75	2.19	4.01	2.69	1.41
GL11	1.56	6.51	2.10	4.16	2.66	1.08
GL12	1.70	6.56	2.10	3.86	2.67	1.10
GL16	3.36	11.06	1.96	3.29	2.58	1.78
GL17	1.69	5.89	1.66	3.48	2.62	0.99
GL19	1.68	6.19	1.65	3.69	2.65	1.02
GL23	2.12	7.59	2.03	3.58	2.68	1.28
GL25	3.15	11.27	1.93	3.57	2.65	1.79
GL28	3.18	10.42	1.87	3.28	2.55	1.66
IV03	2.06	7.27	1.68	3.53	2.49	1.12
IV04	2.19	7.38	1.79	3.36	2.48	1.17
IV05	2.54	7.99	1.66	3.14	2.51	1.30
IV10	3.15	10.22	1.82	3.24	2.47	1.58
IV11	3.42	12.19	1.92	3.56	2.51	1.81
IV12	3.31	10.74	1.87	3.24	2.51	1.68
IV13	3.45	9.29	1.77	3.45	2.43	1.39
IV14	3.25	10.56	1.89	3.24	2.50	1.65
IV15	3.18	10.80	1.90	3.40	2.55	1.69
IV16	3.48	11.17	1.91	3.20	2.52	1.77
IV17	3.33	10.61	1.91	3.18	2.54	1.71

[1]Density derived from measurements on drill cuttings.

References

Combs, J., 1971, Heat flow and geothermal resource estimates for the Imperial Valley, in Rex, R. W., and others, Cooperative geological-geophysical-geochemical investigations of geothermal resources in the Imperial Valley area of California: Riverside, Univ. of California, p. 5-27.

Combs, J., 1972, "Thermal studies," in Rex, R. W., and others, Cooperative investigations of geothermal resources in the Imperial Valley area and their potential value for desalting of water and other purposes: Riverside, Univ. of California, Inst. Geophys. and Planet. Phys., 10 ch., p. B1-B7.

Goss, R., and Combs, J., 1976, Thermal conductivity measurement and prediction from geophysical well log parameters with borehole application, in United Nations Symposium on the Development and Use of Geothermal Resources, 2nd, San Francisco, CA, May 20-29, 1975, Proceedings, v. 2: Lawrence Berkeley Lab., Univ. of California, p. 1019-1027.

Lachenbruch, A. H., Sass, J. H., Galanis, S. P., Jr., and Marshall, B. V., 1983a, Heat flow and crustal extension in the Salton Trough (abs.), in General Assembly, IUGG, XVIII, Hamburg, Germany, August 15-17, 1983, Program and Abstracts, v. 1, p. 504.

Lachenbruch, A. H., Sass, J. H., Galanis, S. P., Jr., and Marshall, B. V., 1983b, Heat flow, crustal extension, and sedimentation in the Salton Trough (abs.): EOS, v. 64, p. 836.

Lachenbruch, A. H., Sass, J. H., and Galanis (?), S. P., Jr., 1984, Heat flow in southernmost California and a simple model for the Salton Trough: Journal of Geophysical Research, in press.

Mase, C. W., Sass, J. H., Brook, C. A., and Munroe, R. J., 1981, Shallow hydrothermal regime of the East Brawley and Glamis KGRA's, Salton Trough, California: U.S. Geological Survey Open-File Report 81-834, 57 p.

Rex, R. W., Babcock, E. A., Biehler, S., Combs, J., Coplen, T. B., Elders, W. A., Furgerson, R. B., Garfunkel, Z., Meidav, T., and Robinson, P. T., 1971, Cooperative geological-geophysical-geochemical investigations of geothermal resources in the Imperial Valley area of California: Riverside, Univ. of California, 153 p.

Sass, J. H., Lachenbruch, A. H., and Munroe, R. J., 1971, Thermal conductivity of rocks from measurements on fragments and its application to heat-flow determinations: Journal of Geophysical Research, v. 71, p. 3391-3401.

Sass, J. H., Kennelly, J. P., Jr., Wendt, W. E., Moses, T. H., Jr., and Ziagos, J. P., 1979, In situ determination of heat flow in unconsolidated sediments: U.S. Geological Survey Open-File Report 79-593, 73 p.

Sass, J. H., Kennelly, J. P., Jr., Wendt, W. E., Moses, T. H., Jr., and Ziagos, J. P., 1981, In-situ determination of heat flow in unconsolidated sediments: Geophysics, v. 46, p. 76-83.

Swanberg, C. A., 1974a, Heat flow and geothermal potential of the East Mesa KGRA, Imperial Valley, California: Conference on Research for the Development of Geothermal Energy Resources, Pasadena, California Inst. Tech., Jet Prop. Lab., Proceedings, p. 85.

Swanberg, C. A., 1974b, Heat-flow studies, in Geothermal resource investigations, East Mesa test site, Imperial Valley, California, status report, November 1974: Boulder City, Nevada, p. 5-6.

Swanberg, C. A., 1976, The Mesa geothermal anomaly, Imperial Valley, California--A comparison and evaluation of results obtained from surface geophysics and deep drilling, in United Nations Symposium on the Development and Use of Geothermal Resources, 2nd, San Francisco, CA, May 20-29, 1975, Proceedings, v. 2: Lawrence Berkeley Lab., Univ. of California, p. 1217-1229.